Occurrence and size distribution study of microplastics in household water from different cities in continental Spain and the Canary Islands

Please, cite as follows:

Virginia Gálvez-Blanca, Carlos Edo, Miguel González-Pleiter, Marina Albentosa, Javier Bayo, Ricardo Beiras, Francisca Fernández-Piñas, Jesús Gago, May Gómez, Rosario Gonzalez-Cascon, Javier Hernández-Borges, Junkal Landaburu-Aguirre, Ico Martínez, Soledad Muniategui-Lorenzo, Cristina Romera-Castillo, Roberto Rosal. Occurrence and size distribution study of microplastics in household water from different cities in continental Spain and the Canary Islands, Water Research, 238, 120044, 2023

https://doi.org/10.1016/j.watres.2023.120044

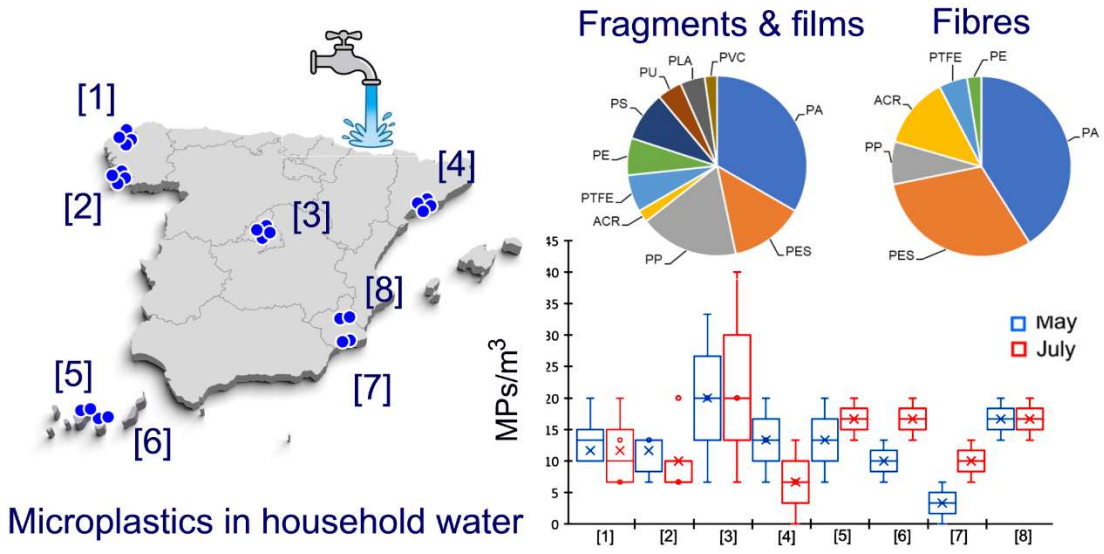

https://www.sciencedirect.com/science/article/pii/S0043135423004803

https://doi.org/10.1016/j.watres.2023.120044

Occurrence and size distribution study of microplastics in household water from different cities in continental Spain and the Canary Islands

Virginia Gálvez-Blanca[1], Carlos Edo[1], Miguel González-Pleiter[2], Marina Albentosa[3], Javier Bayo[4], Ricardo Beiras[5,6], Francisca Fernández-Piñas[2,7], Jesús Gago[8], May Gómez[9], Rosario Gonzalez-Cascon[10], Javier Hernández-Borges[11,12], Junkal Landaburu-Aguirre[13], Ico Martínez[9], Soledad Muniategui-Lorenzo[14], Cristina Romera-Castillo[15], Roberto Rosal[1,*]

[1] Department of Chemical Engineering, Universidad de Alcalá, E-28871 Alcalá de Henares, Madrid, Spain
[2] Department of Biology, Faculty of Science, Universidad Autónoma de Madrid, E-28049, Madrid, Spain
[3] Instituto Español de Oceanografía (IEO-CSIC), Centro Oceanográfico de Murcia, Calle Varadero, 1, 30740, San Pedro del Pinatar, Murcia, Spain
[4] Department of Chemical and Environmental Engineering, Technical University of Cartagena, Paseo Alfonso XIII 44, E-30203, Cartagena, Spain
[5] Centro de Investigación Mariña da Universidade de Vigo (CIM-UVigo), Vigo, Galicia, Spain
[6] Department of Ecology and Animal Biology, University of Vigo, Vigo, Galicia, Spain
[7] Centro de Investigación en Biodiversidad y Cambio Global (CIBC-UAM), Universidad Autónoma de Madrid. C Darwin 2, 28049 Madrid, Spain
[8] Instituto Español de Oceanografía (IEO-CSIC), Centro Oceanográfico de Vigo, Subida a Radio Faro 50, 36390 Vigo, Spain
[9] Grupo de Ecofisiología de Organismos Marinos (EOMAR), IU-ECOAQUA, Universidad de Las Palmas de Gran Canaria, 35017, Las Palmas de Gran Canaria, Canary Islands, Spain
[10] Department of Environment, National Institute for Agriculture and Food Research and Technology (INIA), 28040 Madrid, Spain
[11] Departamento de Química, Unidad Departamental de Química Analítica, Facultad de Ciencias, Universidad de La Laguna (ULL). Avda. Astrofísico Fco. Sánchez, s/n. 38206 San Cristóbal de La Laguna, Spain
[12] Instituto Universitario de Enfermedades Tropicales y Salud Pública de Canarias, Universidad de La Laguna (ULL), Avda. Astrofísico Fco. Sánchez, s/n. 38206 San Cristóbal de La Laguna, Spain
[13] IMDEA Water Institute, Avenida Punto Com, 2, 28805 Alcalá de Henares, Madrid, Spain
[14] University of A Coruña. Grupo Química Analítica Aplicada (QANAP), Instituto Universitario de Medio Ambiente (IUMA), Department of Chemistry. Faculty of Sciences. A Coruña 15071, Spain
[15] Instituto de Ciencias del Mar-CSIC, Paseo Maritimo de la Barceloneta, 37, 08003, Barcelona, Spain

* Corresponding author: roberto.rosal@uah.es

Abstract

The purpose of this study was to investigate the occurrence of microplastics (MPs) in drinking water in Spain by comparing tap water from different locations using common sampling and identification procedures. We sampled tap water from 24 points in 8 different locations from continental Spain and the Canary Islands by means of 25 μm opening size steel filters coupled to household connections. All particles were measured and spectroscopically characterized including not only MPs but also particles consisting of natural materials with evidence of industrial processing, such as dyed natural fibres, referred insofar as artificial particles (APs). The average concentration of MPs was 12.5 ± 4.9 MPs/m^3 and that of anthropogenic particles 32.2 ± 12.5 APs/m^3. The main synthetic polymers detected were polyamide, polyester, and polypropylene, with lower counts of other polymers including the biopolymer poly(lactic acid). Particle size and mass distributions were parameterized by means of power law distributions, which allowed performing estimations of the concentration of smaller particles provided the same scaling parameter of the power law applies. The calculated total mass concentration of the identified MPs was 45.5 ng/L. The observed size distribution of MPs allowed an estimation for the concentration of nanoplastics (< 1 μm) well below the ng/L range; higher concentrations are not consistent with scale invariant fractal fragmentation. Our findings showed that MPs in the drinking water sampled in this work do not represent a significant way of exposure to MPs and would probably pose a negligible risk for human health.

Keywords: Microplastics; Nanoplastics; Drinking water; Particle size distribution; Number concentration; Mass concentration

1. Introduction

Plastic pollution has become ubiquitous and a major cause for concern. With a global production capacity approaching 400 million tonnes per year, the leakage of plastic to the environment has been estimated at 22 million tonnes (OECD, 2022; Plastics Europe, 2022). The obvious reason for the spreading of plastic pollution is the lack of circularity in the current use of plastics. The main contribution is waste mismanagement, with lower inputs from abrasion of plastic goods during use, such as the wearing of tyres and textiles, and pellet losses at production stage (Walker, 2021). Both aquatic and soil ecosystems are a transportation route and sink for most of the plastic that ends up in the environment. Once in the atmosphere, water bodies, and other environments, plastics suffer from uncontrolled mechanical, oxidative, and photochemical degradation that generates smaller and smaller fragments that may reach different environments and interact with the biota and with other particles and substances in a variety of ways (Du et al., 2021). The widespread presence of plastic debris results in risks due to the exposure to chemical additives and to the microorganisms traveling on plastic surfaces as well as a consequence of the possible internalization of small plastic fragments (WHO, 2022). Eventually, plastic particles can reach foods and beverages exposing humans to a new kind of pollution with unknown health implications (van der Laan et al., 2022).

The exposure of humans to microplastics (MPs) is not easy to quantify, making it difficult to identify health risks and to define management policies. Several problems exist for it. The lack of standard procedures, common metrics, and contrasted quality assurance criteria have been widely recognized (Koelmans et al., 2019). The use of different size cutoffs in sampling campaigns contributes to a huge variability among reported results. Specifically concerning drinking water, the results reported in the literature span over orders of magnitude, ranging from a few plastic particles per cubic meter to thousands per litre (Eerkes-Medrano et al., 2019; Mortensen et al., 2021). The exclusive use of number concentration represents an important obstacle for quantifying plastics. The exposure of humans to microplastics in mass concentration units has been estimated in different studies that appeared during last years but conversion from number to mass concentration may lead to huge errors (Pletz, 2022). Besides, the evidence of adverse outcomes from the exposure to plastic debris is still weak due to the difficulty of evaluating sublethal and long-term effects (Rodrigues et al., 2019). Some efforts have been paid to estimate the biodistribution of MPs in humans assuming a certain rate of internalization based on studies performed with engineered nanoparticles, but the current lack of experimental data do not allow to validate model estimations (Mohamed Nor et al., 2021).

The existing data on the occurrence of MPs in drinking water are controversial. Some results from bottled water are particularly high. Oßmann et al. reported concentrations of MPs in mineral water of 2649 ± 2857 MPs/L in polyethylene terephthalate (PET) bottles and even higher, 6292 ± 10521 MPs/L, in glass bottles. Reported MPs in tap water tend to be larger in size and lower in abundance compared to bottled water, but there is a methodological bias due to the use of two different spectroscopic techniques, micro-Raman and micro-FTIR, that differ one order of magnitude in their detection limit (Zhang et al., 2020). In some cases, higher abundances can be probably attributed to the small size sampled thank to the use of micro-Raman (Oßmann et al., 2018; Wang et al., 2020). However, some studies using micro-Raman with the same detection limit, as low as 1 μm, reported relatively low concentrations (Pivokonsky et al., 2020; Schymanski et al., 2018). It has also been suggested that the MPs in drinking water are generally smaller than those found in other food products (Mortensen et al., 2021). There is a general agreement, however in the type of polymers detected, which generally show higher prevalence of the most commonly used materials including polyethylene (PE), polypropylene (PP), polystyrene (PS) and PET (Koelmans et al., 2019; Senathirajah et al., 2021). As expected, a significant fraction of the MPs found in plastic bottles correspond to PET and PP, the materials used for bottles and caps respectively (Schymanski et al., 2018).

The purpose of this study was to compare tap water from different Spanish locations using common sampling and identification procedures. We sampled tap water from 8 different locations in continental Spain and the Canary Islands by means of 25 μm opening size stainless-steel filters coupled to household connections. All particles were measured and spectroscopically characterized including not only plastic particles but also natural materials with evidence of industrial processing, such as dyed natural fibres. Particle size and mass distributions were parameterized by means of power law distributions and the findings discussed and compared with recent data provided by other groups.

2. Materials and methods

2.1. Sampling locations and methodology

Two simultaneous sampling campaigns were performed in 8 different locations in continental Spain and the Canary Islands in spring (May) and summer (July) 2022. The locations chosen consisted of medium-sized towns ranging from San Cristobal de La Laguna (155,000 inhab.) to Murcia (450,000 inhab.) plus the metropolitan areas of Madrid (7.3 million inhab.) and Barcelona (5.5 million inhab.). The sampling points (24) were distributed through the different locations avoiding excessive proximity. The locations and number of sampling points per location are shown in

https://doi.org/10.1016/j.watres.2023.120044

Figure 1. Sampling locations.

Figure 1. Table S1, Supplementary Material (SM), lists the characteristics of the drinking water treatment plants (DWTP) located closer to the sampling points in every location.

A series of 25 µm opening size and 25 µm diameter wire stainless steel filters were adapted into a brass 1/2 in. pipe thread adapter that fitted the usual domestic connectors (Figure S1, SM). The set was prepared in the facilities of Segainvex, Universidad Autónoma de Madrid, and was distributed to the different persons participating in the sampling campaigns. All metal, steel and glass materials were carefully cleaned with Milli-Q water, wrapped with aluminium foil, and heated to 300 ºC for 4 h in order to remove all possible rests of organic matter or any contamination from plastic material or fibres. Prior to sampling, the filter was assembled at the end of domestic bathroom connectors without using any joints. In all samples, 150 L of water were allowed to flow through the filters amounting 3600 L per campaign (7200 L overall). The volume of water was chosen based on a pilot test to avoid filter clogging due to the presence of sand and other particulate material in tap water. After sampling, the filters were disassembled, put inside clean glass Petri dishes, carefully closed, and sent to the laboratory for analyses.

2.2. Analyses

All samples were processed in the same laboratory. Once received, the stainless-steel filters were recovered, washed with Milli-Q water, and the water filtered again using 25 µm stainless steel filters as well as 1 µm glass fibre filters. These measures were intended to recover any plastic that could have migrated from the filters during transportation or could get lost during re-filtration. Subsequently, all filters were stored in Petri dishes and dried at 60 ºC for 24 h for later visualization and analyses. Suspected plastic particles were individually picked up using metal tweezers or a needle, depending on their size, photographed, and measured using a Euromex-Edublue stereomicroscope equipped with Image Focus software, and kept in closed clean containers until spectroscopic characterization. Particles were classified as fibres, fragments, and films. Particles with aspect ratio equal to or greater than 3:1 (as traditionally established for man-made mineral fibres) were considered fibres. If not, they were categorised as fragments except if one dimension was at least one tenth lower than the other two, in which case they were classified as films.

The identification of plastic materials was carried out by means of micro-Fourier Transformed Infrared Spectroscopy (micro-FTIR) using a Perkin-Elmer Spotlight 200i micro-FTIR apparatus equipped with an MCT detector. The micro-FTIR equipment was operated in transmission mode in the 550-4000 cm^{-1} range with spectral resolution 8 cm^{-1}. The selected particles were transferred one by one to KBr discs and spectra were individually recorded. This procedure allowed obtaining high quality spectra for most particles, which were compared with the databases existing in software Omnic 9 (Thermo Scientific) and with our own databases, which have been created with aged plastics of different origins by our group. Pearson correlation was used with a minimum of 65 % matching for positive identification as stated elsewhere (González-Pleiter et al., 2021). All suspected plastic particles found in samples and controls were spectroscopically analysed. The actions taken upon the finding of particles in the controls are explained below.

2.2. Particle size and mass distributions

The abundance of plastic particles in environmental samples has been shown to follow a power law with size (Kooi and Koelmans, 2019). The reason is that fragmentation originates a high number of small particles from a few larger ones (Cózar et al., 2014). Mathematically, the relationship can be expressed by a probability density function denoted as *p(x)*:

$$p(x) = p(x \le X \le x + dx) \propto x^{-\alpha} \qquad [1]$$

where X is the observed value and α the scaling parameter. The scaling parameter has been interpreted as the dimension of a fractal fragmentation process that creates a given distribution and, when followed, the evidence of a scale invariant fragmentation mechanism. The scaling parameter also depends on the fragility (the probability of fragmentation) of the material (Turcotte, 1986). Estimating power-law distributions from experimental data is not trivial. Maximum likelihood estimation (MLE) is the method of choice to avoid large errors in the fitting of experimental data (Clauset et al., 2009). The details on the derivation of the scaling parameter using MLE and bootstrapping for its uncertainty are given as Supplementary Materials. Additional details can be found elsewhere (Gillespie, 2015).

In this work, all MPs were characterized particle by particle based on their two representative projected dimensions: length and width for fragments and films and length and diameter for fibres. The representative size for fragments and films was taken as that of the circle with the same projected area. For fibres, the diameter of the sphere with the same volume as the fibre considered as a cylinder with particle's diameter and length (Happel and Brenner, 2012; Rosal, 2021). For fragments, the volume was estimated as that of sphere with the same projected area, for films assuming that the lowest, non-recorded, dimension was one tenth the lower of the other two, and for fibres the volume of the cylinder with the same diameter and length. The mass of individual particles was estimated using the tabulated average density for each polymer (Table S2, SM).

2.4. Quality assurance & quality control

The measures taken during sampling and laboratory handling to ensure the quality of the data obtained followed the general recommendations stated elsewhere (WHO, 2022). Sample collection was performed by trained personnel belonging to the groups participating in the Spanish Network of Micro- and Nanoplastics in the Environment (www.enviroplanet.net). During all the sampling and processing stages, plastic material was avoided. Filters were sent closed to the sampling points in closed aluminium foil together with two clean Petri Dishes, one for returning the filter, and the other to act as procedural sampling control. Sampling controls were kept open during the sampling procedure, closed afterwards, and returned to the laboratory together with the filter. All material used during sampling and processing was previously cleaned carefully with ultrapure water and heated at 450 °C for 4 h. Shipped materials were covered with aluminium foil also heated to 450 °C for 4 h to remove all possible contamination. Laboratory clothes were made of cotton. During laboratory manipulation, contamination controls consisted of Petri dishes which were kept open during all procedures. In addition, during vacuum filtration processes, 2 L of Milli-Q water were filtered 3 times through a 1 µm filter to assess the contamination of water and laboratory devices. The total number of particles found in controls was 21 (5 fragments and 16 fibres) as detailed in Table S3 (SM). Fragments, films or fibres with the same typology and composition were not considered in the corresponding samples.

3. Results and discussion

3.1. Number concentration and chemical composition

The separation process described before allowed the identification of 570 particles with possible anthropogenic origin. All of them were numbered, photographed, and spectroscopically characterized by micro-FTIR. 84 particles (39 fragments, 6 films and 39 fibres) were positively identified as MPs (synthetic polymers); 132 (7 fragments, 7 films and 118 fibres) were identified as artificial (non-plastic) materials and the rest (360 particles) were natural materials without evidence of anthropogenic processing or particles that could not be identified with the minimum matching established. Artificial particles mainly consisted of cellulose fibres with non-natural colours, regenerated cellulose materials, such as rayon or cellophane, and dyed wool. In what follows such anthropogenic non-plastic materials are denoted as APs standing for artificial particles. Figure 2 shows the concentration measured for MPs (Figure 2a) and artificial particles (AP, Figure 2b) in all sampling locations for the two campaigns performed. (The concentration of fibres and fragments and films are separately given in Fig. S2, SM.) The error bars represent the variability considering the different sampling points studied per location. The average concentrations of MPs and APs, for all locations were 12.5 ± 4.9 MPs/m^3 and 32.2 ± 12.5 APs/m^3.

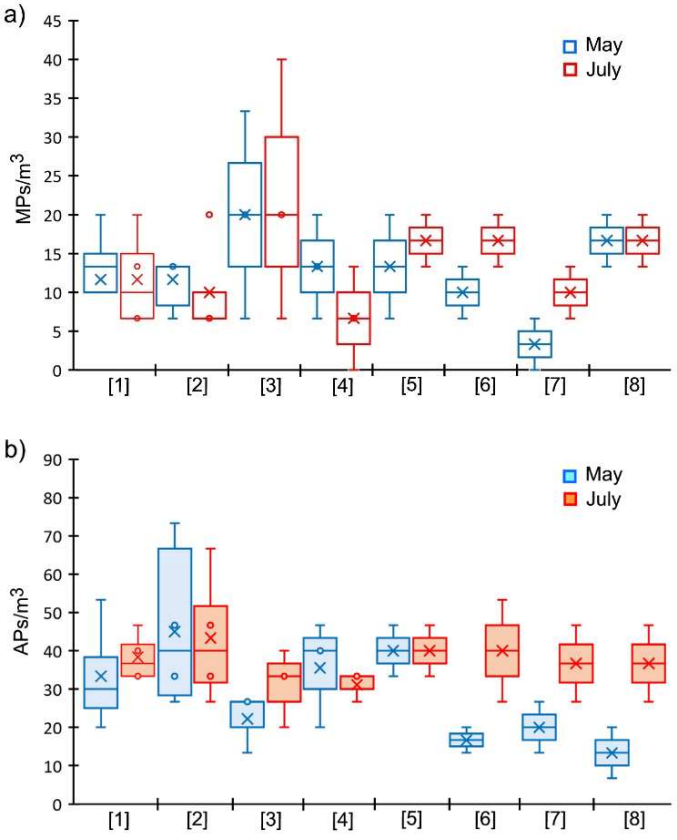

Figure 2. Number concentration of (a) Microplastics [MPs], and (b) Artificial particles [APs] for the different sampling locations. (The variability among samples taken in the same location is given as inclusive quartiles, the bars representing maximum and minimum values; locations as indicated in Figure 1; note that the scale for APs is double than that of MPs.)

As indicated before, there is a large variability in studies reporting the presence of MPs in drinking water. Table 1 summarizes the main details of some recent works on the occurrence of MPs at the outlet of

Table 1. Number concentrations (in MPs/L or MPs/m^3) in drinking water treatment plants (DWTP) and tap water (domestic and end-of-pipe) reported in recent studies.

Place sampled	Reported concentration	Size	Reference
3 DWTPs in urban areas of the Czech Republic	338 ± 76 to 628 ± 28 MPs/L (range)	The size category 1-5 μm represented 40-60% of the total number of MPs	(Pivokonsky et al., 2018)
DWTPs in Lower Saxony (Germany)	< 7 MPs/m^3 (average 0.7 MPs/m^3)	Particle sizes in the 50-150 μm range	(Mintenig et al., 2019)
2 DWTPs in the Czech Republic	14 ± 1 MPs/L and 151 ± 4 MPs/L	1-5 μm accounted for 50-65% of fragments. No fibres < 10 μm	(Pivokonsky et al., 2020)
38 end-of-pipe samples of tap water from different cities in China	0-1247 MPs/L, mean 440 MPs/L	3 μm to 4.45 mm, average 66 μm	(Tong et al., 2020)
8 DWTP in England and Wales, United Kingdom	4.9 MPs/L (average, inlet water) and < 0.11 MP/m^3 (outlet)	Microplastics ≥ 25 μm	(Johnson et al., 2020)
A large DWTP is the Yangtze River Delta, China	930 ± 71 MPs/L	1–5 μm represented > 85%	(Wang et al., 2020)
3 conventional DWTPs in Tehran, Iran	971-1401 MPs/L	almost all plastics > 50 μm	(Adib et al., 2021)
One DWTP in Spain using sand filtration, GAC and Reverse osmosis	0.96 ± 0.46 MPs/L (inlet) 0.06 ± 0.04 MPs/L outlet	In treated water 13 fragments (75 x 138 μm the smaller one) and 16 fibres	(Dalmau-Soler et al., 2021)
Conventional DWTP in Geneva, Switzerland	19.5 to 143.5 MPs/m^3 (inlet water) and < 8 MP/m^3 (outlet)	MPs and synthetic fibres with sizes ≥ 63 μm	(Negrete Velasco et al., 2022)
3 DWTPs in the Paris region with conventional and membrane treatments	7.4 to 5.0 MP/L (inlet water) and < 260 MP/m^3 (outlet)	25–5,000 μm	(Barbier et al., 2022)
One DWTP and its distribution system in Tianjin, China	95.6 MPs/L at the outlet and [lower] 13.2 MPs/L in tap water	> 200 μm predominated in raw water, 100-200 μm in tap water	(Chu et al., 2022)
8 DWTP in Flanders, Belgium and tap water from 5 locations	0.02 ± 0.03 MPs/L (DWTP) and 0.01 ± 0.02 MPs/L (tap water)	50–75 μm represented 44% of the particles, average size 140 ± 271 μm	(Semmouri et al., 2022)

drinking water treatment plants (DWTP) or at the end of distribution systems including houses and other end-of-pipe users. Mintenig et al. obtained an average concentration of 0.7 MPs/m^3 (ranging from 0 to 7 MPs/m^3) in the area covered by Oldenburg-East-Frisian water board (Lower Saxony, Germany) all of them in the 50-150 μm size range (Mintenig et al., 2019). Semmouri et al. studied the presence of MPs (25–1000 μm) in drinking water from different DWTPs in Flanders (Belgium), a highly urbanized region, and reported number concentrations in the tens of MPs per cubic meter range (Semmouri et al., 2022). Weber et al. sampled the drinking water of a German city sampled in 8 end-of-pipe points and one transfer station and found number concentrations < 7 MPs/m^3 (Weber et al., 2021). Incidentally, Weber et al. used micro-Raman spectrometry with 10 μm detection limit, and a methodology similar to that used in other works reporting much higher concentrations of MPs. Barbier et al. studied DWTPs using conventional treatments in the region of Paris plus one implementing microfiltration and nanofiltration. The authors found concentrations < 260 MP/m^3 at the outlet with high removal efficiency (> 99%) with respect to inlet water. Incidentally, the outlet of the plant using membrane processes did not show plastic above blank levels (Barbier et al., 2022). Other studies in conventional DWTPs showed low concentrations of MPs, in the order of a few MPs/m^3 or lower (Johnson et al., 2020; Negrete Velasco et al., 2022).

Other results, however, report much higher concentration of MPs. Chu et al. sampled one DWTP and its distribution system and found concentrations ranging from 13.2 to 134.8 MPs/L, with sizes generally > 200 µm. Surprisingly, the concentration observed in tap water was lower than that recorded at the exit of the DWTP (13.2 MPs/L versus 95.6 MPs/L), which is probably the consequence of sample inhomogeneity or the mixture of tap water from different DWTPs (Chu et al., 2022). In another study performed in several Chinese cities, an average 440 MPs/L was obtained (although some samples did not contain any MPs) with an average size of 66 µm, mostly fragments, and the most abundant size category being 1-50 µm (Tong et al., 2020). Also in the upper range, Pivonkonsky et al. sampled DWTPs in the Czech Republic and reported number concentrations in the 4 ± 1 MPs/L to 628 ± 28 MPs/L, the most abundant size category corresponding to the smaller particles, 1-5 µm (Pivokonsky et al., 2018; Pivokonsky et al., 2020). The differences among reported concentrations may be caused by several factors, that include the use of too small sample volumes, inadequate methodologies for determining MPs or the improper use of blanks and contamination controls, but other probable reasons are the different characteristics of the source water and the different type of treatment technologies used in DWTPs.

The composition of the particles found in our study was dominated by common polymers as shown in Figure 3. The most frequently found were polyamide (PA) and polyester (PES, which include PET), both predominant in fibres, and PP. These three polymers accounted for > 70% of the total number of MPs found in this study. Other polymers detected in lower amounts were acrylic materials (ACR), polytetrafluoroethylene (PTFE), PE, PS, polyurethane (PU), polyvinyl chloride (PVC) and, noticeably, the biopolymer polylactic acid (PLA), which is reported in drinking water by the first time. Figure S2 (SM) shows pictures and FTIR spectra of a PES fragment, an ACR fibre and a PLA fragment. The predominance of PA, PES, and the polyolefins PE and PP agrees well with others' results (Koelmans et al., 2019; Menon et al., 2023; Mintenig et al., 2019; Pivokonsky et al., 2018; Senathirajah et al., 2021; Tong et al., 2020). Figure 2b shows the number concentration of artificial non-plastic pollutants, which was in the 13.3-43.3 APs/m^3 range. The materials included in this category exclude MPs and consist of a wide range of artificial particles. The most abundant class is that of industrially processed natural polymers like regenerated cellulose and a variety of natural materials that underwent industrial processing such as fibres from cotton or wool textiles as revealed by non-natural colours. Most of these artificial materials are fibres (89.4 %) mainly of cellulosic composition (> 85 %). Such artificial particles are generally sampled together with MPs and share some of their characteristics. Specifically, the textile industry uses a wide variety of additives for a number of different functions that become dispersed into the environment upon landfilling or after fibre detaching from clothes during use or washing. Chemicals of concern include persistent and bioaccumulable compounds such as ultraviolet filters, brominated compounds, or perfluorocarbon additives (Darbra et al., 2012). Besides, some characteristics of processed fibres like hydrophobicity and microroughness favour the attachment of microorganisms, which find a way to spread thanks to the high mobility of individual fibres (Stanton et al., 2019; Varshney et al., 2021). The contamination with this type of artificial materials has been seldom reported in the literature (González-Pleiter et al., 2021; Pivokonsky et al., 2020).

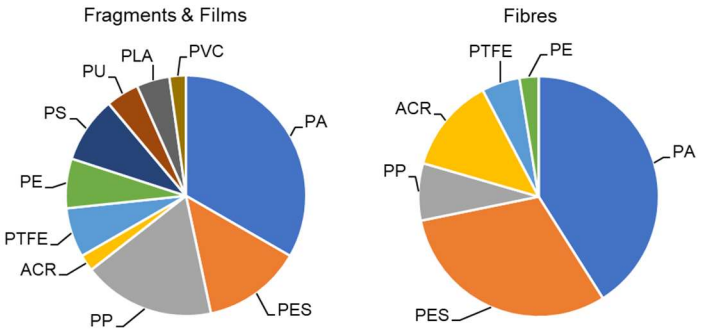

Figure 3. Chemical composition of fragments/films and fibres for the (84) particles spectroscopically identified as MPs by micro-FTIR. (PA: polyamide; PES: polyester; PP: polypropylene; PE: polyethylene; PTFE: polytetrafluoroethylene; ACR: acrylic polymers; PS: polystyrene; PU: polyurethane; PLA: polylactic acid, PVC: polyvinyl chloride.)

The total concentration of microplastics (from all sampled sizes from 41.0 µm to 379.5 µm, the largest sampled MP particle) could be computed from the recorded dimensions of plastic particles and the density of each polymer. The total concentration of the MPs sampled in this study was 45.5 ng/L calculated from the estimated particle volume and the tabulated average density for each polymer as indicated in Table S2. For this calculation, fragments were assumed spherical with the diameter as the sphere with the same projected area, for films slab shape assuming that the non-recorded dimension was one tenth the lower recorded, and for fibres cylindrical shape. The experimental mass concentration of MPs corresponds to usual concentration range reported for other micropollutants in water resources. This includes pesticides, other persistent chemicals and pharmaceuticals and personal care products (Tröger et al., 2018). Some studies reported mass concentration instead of the usual number concentration for MPs in drinking water. Gomiero et al. used pyrolysis gas chromatography-mass spectrometry (Pyr-GC/MS) to analyse the content of

NPs (< 1 µm) in the drinking water from a medium-sized Norwegian city and reported a total mass concentration in the 6.1-93.1 ng/L range, in line with our results (Gomiero et al., 2021). Kirstein et al. tracked MPs down to 6.6 µm in drinking water distribution systems by micro-FTIR and Pyr-GC/MS and found average MPs concentrations between zero and 22 ± 19 MPs/m^3 and mass concentrations in the 0.14-5.43 µg/L (Kirstein et al., 2021).

3.2. Particle size distributions

Particle size distributions for all the MPs sampled in this work is given in Figure 4 as CFD plots for size and mass. The results showed that the power law can be applied for the lower sizes (and separately for the larger ones). The boundary was established using MLE as indicated before. The last particle for which the power law was applied included was a PES fragment of 192.7 µm and 5.2 µg. The scaling parameter, $\hat{\alpha}$, was 1.78 ± 0.14 for particle size and 1.25 ± 0.10 for particle mass. The intervals represent 95% confidence intervals calculated using bootstrapping with n = 50. It is to be noted that the environmental concentrations documented so far in marine studies also follow a power law with exponents ~1.6 as determined elsewhere (Kooi and Koelmans, 2019).

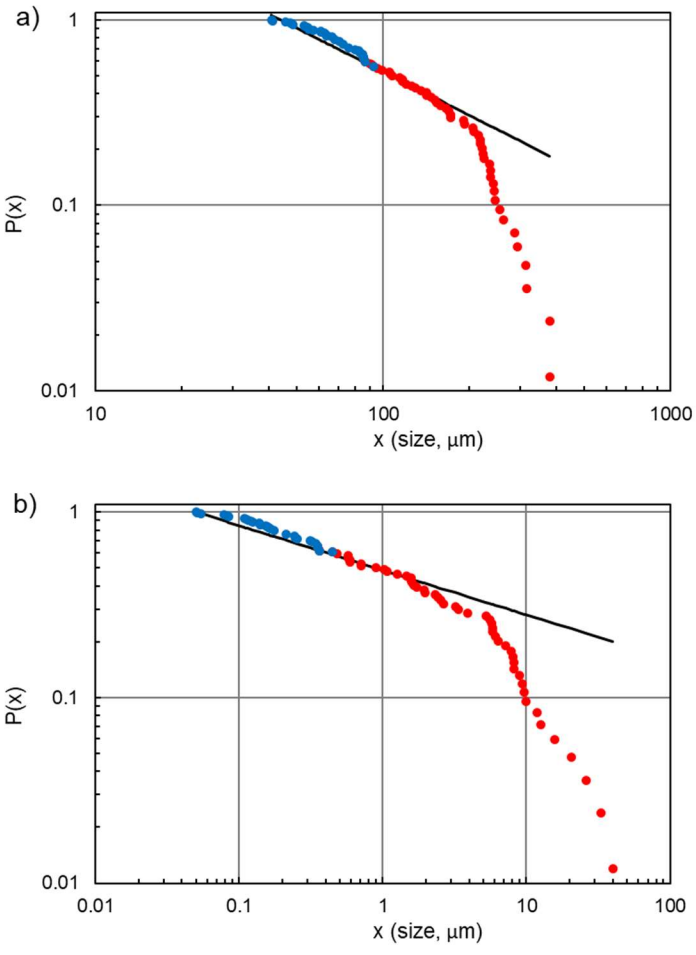

Figure 4. Particle size distributions as CFD. *P(size > x)* (a) and *P(mass > m)* (b). (Red, fragments and films; blue, fibres.)

It has been shown that in some cases, the experimental data on MPs abundance follow a power law distribution only for sizes above a given lower boundary (Cózar et al., 2014). In such cases particle size distributions (as number distributions or as probability density function) usually display a maximum, with a lower number of small particles than expected if all the distribution followed the same power law. The maximum corresponds to different sizes depending on the study, a fact that has been attributed to the difficulty of counting small particles or other variables like the distance to the nearest coast (Kaandorp et al., 2021). In our case, the power law behaviour applies for all particles < 192.7 µm or < 5.2 µg, which allows performing estimations about the number and mass of particles in different size or mass ranges. The procedure is based on the integration of the size distribution function, which is obtained from the density function, *p(x)* as follows:

$$n(x) = N\ p(x) \qquad [2]$$

Where *N* is total number (or number concentration) of particles and *n(x)* the number of particles with sizes between *x* and *x* + *dx*. The mass of every individual particle is calculated from its equivalent diameter and the density of each polymer. The details of the derivation are given as Supplementary Materials. Using the experimental data from our study (the mass or particles between 40.9 µm, the smaller one, and 192.7 µm, calculated as 55.1 µg), the mass for other size ranges can be estimated, even outside the experimental range by extrapolation to lower sizes assuming the same scaling parameter (1.78 ± 0.14) can be applied. Our results predicted 1.8 (1.7-2.0) ng/L for particles < 100 µm, but only 68 (31-140) fg/L for nanoplastics (NPs, < 1 µm) with boundaries calculated using the uncertainty of the scaling parameter.

It is well-established that a series of entities satisfying Eq. 1 define a fractal, the dimension of which is the exponent of its number-size distribution (Turcotte, 1986). A fragmentation process that gives rise to a fractal distribution is taken as evidence of scale invariance. This means that fragments behave in a similar way was as parent particles or, in other words, they constitute a fractal because all parts are similar to the whole (Xu, 2005). Fractal fragmentation approaches based on multi-step iterations foresee that the slope should approach 3 (in 3D fragmentation) as the probability of fragmentation increases. Therefore, the slope relating the number of fragments with their size in double logarithmic coordinate system depends on the dimensionality of the fragmentation process and on the probability of fracturing, which in turn depends on the fragility of the material. A change in slope may mean a change in fractal dimension of in the probability of fragmentation, but there are other possibilities. For example, the action of mechanisms draining small particles (ingestion) or large particles (sedimentation).

Also, numerical bias due to the influence of a few large fragments. The exact reason is still not clear and requires further studies.

MPs break down eventually giving rise to nanoplastics (NPs), which may induce toxicity after their internalization in living organisms and their cells. Li et al. studied the presence of NPs of different sizes (< 450 nm) in tap water and quantified them using Pyr-GC/MS. The reported abundance for the size range 58–255 nm was 1.67–2.08 μg/L (Li et al., 2022). Pyr-GC/MS is a complex technique still under development and the results are scarce and difficult to compare. Xu et al. studied the presence of six synthetic polymers in ultrafiltrated (100 kDa, approx. 10 nm) surface water and groundwater and reported mass concentrations from 21 ng/L to 0.793 μg/L (Xu et al., 2022). Even if the scaling parameter reached 3, the limit of high fracture probability in 3D fragmentation, our set of observed data would yield ∼5 ng/L (x < 100 μm) or ∼50 pg/L (x < 1 μm). From particle mass distribution (Figure 2b) the total mass concentration of particles < 5 μg would be 8.6 ng/L in line with the estimations based on particle size distribution. Therefore, our results suggest that the concentrations of NPs in drinking water should be much below the ng/L level to be consistent with scale invariant fractal fragmentation, which would predict concentrations several orders of magnitude lower, in the tens of pg/L level or less. This is true not only for the concentration of MPs observed in this study, but for most reported in the literature. Higher concentrations of NPs can only be explained by some process that concentrates NPs, or assuming NPs are directly produced from larger plastic particles following a non-fractal mechanism. In both cases, the power law would not apply to NPs, and the abundance of NPs would contradict the general assumption that small plastic fragments interact preferably with the biota and with other particles so that their concentration should be lower than expected from a scale invariant fragmentation pattern. However, this discussion is far to be closed because the fate of NPs in aqueous matrixes is still poorly known and requires more research efforts.

The median MP concentration in untreated water sources was estimated in the thousands of particles per cubic meter with sizes usually > 50 μm (Li et al., 2020). The removal efficiency of MPs DWTPs using traditional technologies, which include coagulation-flocculation, sedimentation, and sand filtration, is generally high, typically 60-80 % (Pivokonsky et al., 2018). Coagulation-sedimentation alone has a removal efficiency of about 50 % and performed better for the removal of fibres (Wang et al., 2020). Granular activated carbon (GAC) filtration is more efficient for small-sized MPs so that MPs > 10 μm are not expected to be found in the effluents of sand filtration (Dalmau-Soler et al., 2021). Oxidation processes such as ozonation may increase the abundance of small (1–5 μm) MPs probably due to the fragmentation of larger particles (Cheng et al., 2021). Membrane filtration, although more expensive is the preferred process to remove very small MPs and NPs from drinking water (Barbier et al., 2022; Shen et al., 2020). Our results included locations receiving water from desalination plants (Table S1, SM, locations 4 and 6) did not show significant differences with other locations in which DWTPs do not use membrane processes. The fact that water treated by ultrafiltration/reverse osmosis still contains MPs has been noticed elsewhere and can be attributed to operational reasons, like plastic unintentionally added during remineralization or plastic detached from polymeric membranes (Dalmau-Soler et al., 2021). In our study, the highest concentration of MPs (77 MPs/m^3) were obtained in tap water from a town receiving drinking water from the DWTP of Santillana (Madrid) that takes water from the same reservoir that receives wastewater at a distance of just 4 km. This situation is common as most DWTPs in our study take water from rivers or reservoirs receiving discharges from WWTPs. In this work, we did not find any relationship between plastic concentration and water quality parameters including the use of water desalted by reverse osmosis. Our results suggest that the quality of water discharged by wastewater treatment plants is an important parameter influencing that of the drinking water produced after potabilization processes.

According to our study and considering a daily consumption of 1.5 L of tap water per day, the annual intake would represent 6.8 MPs per person and per year and per person with a global weight of 24.9 μg, and somewhat higher amount of artificial fibres (17.6 per person and per year, mainly dyed natural fibres and regenerated cellulose). Our results showed that tap water delivered by DWTPs and conventional distribution systems under study do not represent a significant way of exposure to MP pollution and would probably pose a low risk for human health. However, it is true that the actual concentrations of MPs and NPs in drinking water are controversial because of reports differing orders of magnitude. Although part of the differences could be attributed to methodological reasons, a high variability due to differences in water sources cannot be discarded. Besides, the risks associated to MPs in drinking are complex and can also be due to the increased exposure to pathogenic colonizing microorganisms including the transmission of antibiotic resistance genes, to the internalization and possible accumulation of NPs (particles small enough to cross epithelial barriers), and to the exposure to chemicals used as additives in the formulation of plastic materials (Martínez-Campos et al., 2021).

4. Conclusions

MPs have received increasing attention as emerging pollutants in drinking water. However, the dispersion of results and methodological discrepancies among studies make it difficult to derive conclusions on their possible

effects and risks for human health. Herein, we performed an estimation of the total amount on plastic in drinking water, both in number and mass concentration from the municipal water supply of eight locations in continental Spain and the Canary Islands.

Our results allowed identifying 10 types of synthetic polymers, the most abundant of which were PA, PES, PP, and with lower counts, ACR, PE, PTFE, PS, PU, PVC, and notably, the biopolymer PLA. We also identified other anthropogenic materials mainly consisting of cellulose fibres with non-natural colours and regenerated cellulose materials, such as rayon or cellophane. The average concentration of MPs was 12.5 ± 4.9 MPs/m^3 and that of other artificial particles 32.2 ± 12.5 APs/m^3.

The particles identified as MPs displayed sizes in the 41.0-379.5 μm range with a calculated total mass concentration of 45.5 ng/L. Particle size and mass distributions followed a power law for sizes < 192.7 μm, which allowed performing estimations for the concentration of smaller particles provided the same scaling parameter of the power law applies. The scaling parameter can be interpreted as the dimension of the fragmentation process. Based on this assumption, the concentration of NPs would be extremely low, far below the ng/L range.

Our results showed that MPs in drinking water do not represent a significant way of exposure to MPs and would probably pose a low risk for human health. Besides, results reporting concentrations of NPs in drinking water in the ng/L level are not consistent with scale invariant fractal fragmentation, given the observed size distribution for MPs.

Acknowledgements

The authors acknowledge the support provided by Spanish Network of Plastics in the Environment, EnviroPlaNet (www.enviroplanet.net). The authors acknowledge the financial support provided by Plastics Europe and that of the Spanish Government, Ministerio de Ciencia e Innovación, grants PID2020-113769RB-C21/C22. The authors would like to thank the Interdepartmental Investigation Research Service of the Universidad Autónoma de Madrid (SIDI-UAM and Segainvex) for the use of their infrastructures and their technical support. The authors gratefully acknowledge Pilar Jiménez, Joaquín López-Castellanos, Rebeca Mallenco, Natàlia Timoneda, Massimo Pernice, Judith Traver and Claudia Valle for their assistance with the collection of water samples.

References

Adib D, Mafigholami R, Tabeshkia H. Identification of microplastics in conventional drinking water treatment plants in Tehran, Iran. Journal of Environmental Health Science and Engineering 2021; 19: 1817-1826.

Barbier J-S, Dris R, Lecarpentier C, Raymond V, Delabre K, Thibert S, Tassin B, Gasperi J. Microplastic occurrence after conventional and nanofiltration processes at drinking water treatment plants: Preliminary results. 2022; 4.

Cheng YL, Kim J-G, Kim H-B, Choi JH, Tsang YF, Baek K. Occurrence and removal of microplastics in wastewater treatment plants and drinking water purification facilities: A review. Chemical Engineering Journal 2021; 410.

Chu X, Zheng B, Li Z, Cai C, Peng Z, Zhao P, Tian Y. Occurrence and distribution of microplastics in water supply systems: In water and pipe scales. Science of The Total Environment 2022; 803: 150004.

Clauset A, Rohilla-Shalizi C, Newman MEJ. Power-Law distributions in empirical data. SIAM Review 2009; 51: 661-703.

Cózar A, Echevarría F, González-Gordillo JI, Irigoien X, Úbeda B, Hernández-León S, Palma ÁT, Navarro S, García-de-Lomas J, Ruiz A, Fernández-de-Puelles ML, Duarte CM. Plastic debris in the open ocean. 2014; 111: 10239-10244.

Dalmau-Soler J, Ballesteros-Cano R, Boleda MR, Paraira M, Ferrer N, Lacorte S. Microplastics from headwaters to tap water: occurrence and removal in a drinking water treatment plant in Barcelona Metropolitan area (Catalonia, NE Spain). Environmental Science and Pollution Research 2021; 28: 59462-59472.

Darbra RM, Dan JRG, Casal J, Àgueda A, Capri E, Fait G, Schuhmacher M, Nadal M, Rovira J, Grundmann V, Barceló D, Ginebreda A, Guillén D. Additives in the textile industry. In: Bilitewski B, Darbra RM, Barceló D, editors. Global Risk-Based Management of Chemical Additives I: Production, Usage and Environmental Occurrence. Springer Berlin Heidelberg, Berlin, Heidelberg, 2012, pp. 83-107.

Du S, Zhu R, Cai Y, Xu N, Yap P-S, Zhang Y, He Y, Zhang Y. Environmental fate and impacts of microplastics in aquatic ecosystems: a review. RSC Advances 2021; 11: 15762-15784.

Eerkes-Medrano D, Leslie HA, Quinn B. Microplastics in drinking water: A review and assessment. Current Opinion in Environmental Science & Health 2019; 7: 69-75.

Gillespie CS. Fitting heavy tailed distributions: The poweRlaw package. Journal of Statistical Software 2015; 64: 1 - 16.

Gomiero A, Oysaed KB, Palmas L, Skogerbo G. Application of GC/MS-pyrolysis to estimate the levels of microplastics in a drinking water supply system. Journal of Hazardous Materials 2021; 416.

González-Pleiter M, Edo C, Aguilera Á, Viúdez-Moreiras D, Pulido-Reyes G, González-Toril E, Osuna S, de Diego-Castilla G, Leganés F, Fernández-Piñas F, Rosal R. Occurrence and

transport of microplastics sampled within and above the planetary boundary layer. Science of The Total Environment 2021; 761: 143213.
Happel J, Brenner H. Low Reynolds number hydrodynamics: with special applications to particulate media (Vol. 1): Springer Science & Business Media, 2012.
Johnson AC, Ball H, Cross R, Horton AA, Jürgens MD, Read DS, Vollertsen J, Svendsen C. Identification and Quantification of Microplastics in Potable Water and Their Sources within Water Treatment Works in England and Wales. Environmental Science & Technology 2020; 54: 12326-12334.
Kaandorp MLA, Dijkstra HA, van Sebille E. Modelling size distributions of marine plastics under the influence of continuous cascading fragmentation. Environmental Research Letters 2021; 16: 054075.
Kirstein IV, Hensel F, Gomiero A, Iordachescu L, Vianello A, Wittgren HB, Vollertsen J. Drinking plastics? - Quantification and qualification of microplastics in drinking water distribution systems by mu FTIR and Py-GCMS. Water Research 2021; 188.
Koelmans AA, Nor NHM, Hermsen E, Kooi M, Mintenig SM, De France J. Microplastics in freshwaters and drinking water: Critical review and assessment of data quality. Water Research 2019; 155: 410-422.
Kooi M, Koelmans AA. Simplifying microplastic via continuous probability distributions for size, shape, and density. Environmental Science & Technology Letters 2019; 6: 551-557.
Li Y, Li W, Jarvis P, Zhou W, Zhang J, Chen J, Tan Q, Tian Y. Occurrence, removal and potential threats associated with microplastics in drinking water sources. Journal of Environmental Chemical Engineering 2020; 8.
Li Y, Wang Z, Guan B. Separation and identification of nanoplastics in tap water. Environmental Research 2022; 204: 112134.
Martínez-Campos S, González-Pleiter M, Fernández-Piñas F, Rosal R, Leganés F. Early and differential bacterial colonization on microplastics deployed into the effluents of wastewater treatment plants. Science of The Total Environment 2021; 757: 143832.
Menon V, Sharma S, Gupta S, Ghosal A, Nadda AK, Jose R, Sharma P, Kumar S, Singh P, Raizada P. Prevalence and implications of microplastics in potable water system: An update. Chemosphere 2023: 137848.
Mintenig SM, Loeder MGJ, Primpke S, Gerdts G. Low numbers of microplastics detected in drinking water from ground water sources. Science of the Total Environment 2019; 648: 631-635.
Mohamed Nor NH, Kooi M, Diepens NJ, Koelmans AA. Lifetime accumulation of microplastic in children and adults. Environmental Science & Technology 2021; 55: 5084-5096.
Mortensen NP, Fennell TR, Johnson LM. Unintended human ingestion of nanoplastics and small microplastics through drinking water, beverages, and food sources. Nanoimpact 2021; 21.
Negrete Velasco A, Ramseier Gentile S, Zimmermann S, Stoll S. Contamination and Removal Efficiency of Microplastics and Synthetic Fibres in a Conventional Drinking Water Treatment Plant. 2022; 4.
OECD. Global Plastics Outlook, 2022.
Oßmann BE, Sarau G, Holtmannspötter H, Pischetsrieder M, Christiansen SH, Dicke W. Small-sized microplastics and pigmented particles in bottled mineral water. Water Research 2018; 141: 307-316.
Pivokonsky M, Cermakova L, Novotna K, Peer P, Cajthaml T, Janda V. Occurrence of microplastics in raw and treated drinking water. Scence of the Total Environment 2018; 643: 1644-1651.
Pivokonsky M, Pivokonska L, Novotna K, Cermakova L, Klimtova M. Occurrence and fate of microplastics at two different drinking water treatment plants within a river catchment. Science of the Total Environment 2020; 741.
Plastics Europe. Plastics—The Facts 2022: An Analysis of European Plastics Production, Demand and Waste Data. PlasticsEurope; Association of Plastics Manufacturers, Brussels, 2022.
Pletz M. Ingested microplastics: Do humans eat one credit card per week? Journal of Hazardous Materials Letters 2022; 3: 100071.
Rodrigues MO, Abrantes N, Gonçalves FJM, Nogueira H, Marques JC, Gonçalves AMM. Impacts of plastic products used in daily life on the environment and human health: What is known? Environmental Toxicology and Pharmacology 2019; 72: 103239.
Rosal R. Morphological description of microplastic particles for environmental fate studies. Marine Pollution Bulletin 2021; 171: 112716.
Schymanski D, Goldbeck C, Humpf H-U, Fürst P. Analysis of microplastics in water by micro-Raman spectroscopy: Release of plastic particles from different packaging into mineral water. Water Research 2018; 129: 154-162.
Semmouri I, Vercauteren M, Van Acker E, Pequeur E, Asselman J, Janssen C. Presence of microplastics in drinking water from different freshwater sources in Flanders (Belgium), an urbanized region in Europe. International Journal of Food Contamination 2022; 9: 6.
Senathirajah K, Attwood S, Bhagwat G, Carbery M, Wilson S, Palanisami T. Estimation of the mass of microplastics ingested – A pivotal first step towards human health risk assessment. Journal of Hazardous Materials 2021; 404: 124004.
Shen M, Song B, Zhu Y, Zeng G, Zhang Y, Yang Y, Wen X, Chen M, Yi H. Removal of microplastics

via drinking water treatment: Current knowledge and future directions. Chemosphere 2020; 251.
Stanton T, Johnson M, Nathanail P, MacNaughtan W, Gomes RL. Freshwater and airborne textile fibre populations are dominated by 'natural', not microplastic, fibres. Science of The Total Environment 2019; 666: 377-389.
Tong H, Jiang Q, Hu X, Zhong X. Occurrence and identification of microplastics in tap water from China. Chemosphere 2020; 252: 126493.
Tröger R, Klöckner P, Ahrens L, Wiberg K. Micropollutants in drinking water from source to tap - Method development and application of a multiresidue screening method. Science of The Total Environment 2018; 627: 1404-1432.
Turcotte DL. Fractals and fragmentation. 1986; 91: 1921-1926.
van der Laan LJW, Bosker T, Peijnenburg WJGM. Deciphering potential implications of dietary microplastics for human health. Nature Reviews Gastroenterology & Hepatology 2022.
Varshney S, Sain A, Gupta D, Sharma S. Factors affecting bacterial adhesion on selected textile fibres. Indian Journal of Microbiology 2021; 61: 31-37.
Walker TR. (Micro)plastics and the UN Sustainable Development Goals. Current Opinion in Green and Sustainable Chemistry 2021; 30: 100497.
Wang Z, Lin T, Chen W. Occurrence and removal of microplastics in an advanced drinking water treatment plant (ADWTP). Science of the Total Environment 2020; 700.
Weber F, Kerpen J, Wolff S, Langer R, Eschweiler V. Investigation of microplastics contamination in drinking water of a German city. Science of the Total Environment 2021; 755.
WHO. Dietary and inhalation exposure to nano-and microplastic particles and potential implications for human health. World Health Organization, 2022.
Xu Y. Explanation of scaling phenomenon based on fractal fragmentation. Mechanics Research Communications 2005; 32: 209-220.
Xu Y, Ou Q, Jiao M, Liu G, van der Hoek JP. Identification and quantification of nanoplastics in surface water and groundwater by pyrolysis gas chromatography–mass spectrometry. Environmental Science & Technology 2022; 56: 4988-4997.
Zhang Q, Xu EG, Li J, Chen Q, Ma L, Zeng EY, Shi H. A Review of microplastics in table salt, drinking water, and air: Direct human exposure. Environmental Science & Technology 2020; 54: 3740-3751.

Supplementary Material

Occurrence and size distribution study of microplastics in household water from different cities in continental Spain and the Canary Islands

Virginia Gálvez-Blanca[1], Carlos Edo[1], Miguel González-Pleiter[2], Marina Albentosa[3], Javier Bayo[4], Ricardo Beiras[5,6], Francisca Fernández-Piñas[2,7], Jesús Gago[8], May Gómez[9], Rosario Gonzalez-Cascon[10], Javier Hernández-Borges[11,12], Junkal Landaburu-Aguirre[13], Ico Martínez[9], Soledad Muniategui-Lorenzo[14], Cristina Romera-Castillo[15], Roberto Rosal[1]

[1] Department of Chemical Engineering, Universidad de Alcalá, E-28871 Alcalá de Henares, Madrid, Spain
[2] Department of Biology, Faculty of Science, Universidad Autónoma de Madrid, E-28049, Madrid, Spain
[3] Instituto Español de Oceanografía (IEO-CSIC), Centro Oceanográfico de Murcia, Calle Varadero, 1, 30740, San Pedro del Pinatar, Murcia, Spain
[4] Department of Chemical and Environmental Engineering, Technical University of Cartagena, Paseo Alfonso XIII 44, E-30203, Cartagena, Spain
[5] Centro de Investigación Mariña da Universidade de Vigo (CIM-UVigo), Vigo, Galicia, Spain
[6] Department of Ecology and Animal Biology, University of Vigo, Vigo, Galicia, Spain
[7] Centro de Investigación en Biodiversidad y Cambio Global (CIBC-UAM), Universidad Autónoma de Madrid. C Darwin 2, 28049 Madrid, Spain
[8] Instituto Español de Oceanografía (IEO-CSIC), Centro Oceanográfico de Vigo, Subida a Radio Faro 50, 36390 Vigo, Spain
[9] Grupo de Ecofisiología de Organismos Marinos (EOMAR), IU-ECOAQUA, Universidad de Las Palmas de Gran Canaria, 35017, Las Palmas de Gran Canaria, Canary Islands, Spain
[10] Department of Environment, National Institute for Agriculture and Food Research and Technology (INIA), 28040 Madrid, Spain
[11] Departamento de Química, Unidad Departamental de Química Analítica, Facultad de Ciencias, Universidad de La Laguna (ULL). Avda. Astrofísico Fco. Sánchez, s/n. 38206 San Cristóbal de La Laguna, Spain.
[12] Instituto Universitario de Enfermedades Tropicales y Salud Pública de Canarias, Universidad de La Laguna (ULL), Avda. Astrofísico Fco. Sánchez, s/n. 38206 San Cristóbal de La Laguna, Spain.
[13] IMDEA Water Institute, Avenida Punto Com, 2, 28805 Alcalá de Henares, Madrid, Spain
[14] University of A Coruña. Grupo Química Analítica Aplicada (QANAP), Instituto Universitario de Medio Ambiente (IUMA), Department of Chemistry. Faculty of Sciences. A Coruña 15071, Spain
[15] Instituto de Ciencias del Mar-CSIC, Paseo Maritimo de la Barceloneta, 37, 08003, Barcelona, Spain

https://doi.org/10.1016/j.watres.2023.120044

Table S1. Technologies used in the closest DWTPs to the end-of-pipe points sampled.

Sampling point	DWTP	Capacity	Technology
[1] Coruña	La Telva	2.4 m^3/s	Coagulation with PAC and $Al_2(SO_4)_3$, oxidation with $KMnO_4$, sand filtration, and chlorination (Cl_2)
[2] Vigo	Casal	1.5 m^3/s	Prechlorination, sedimentation, ozonation (optional), sand filtration, and chlorination with Cl_2
[2] Vigo	Valladares	0.2 m^3/s	Prechlorination witn NaClO, coagulation/flocculation (optional), sedimentation, sand filtration, and chlorination with NaClO
[3] Madrid	Colmenar Viejo	16 m^3/s	Preoxidation-prechlorination (Cl_2 and Cl_2O), coagulation with PAC, flocculation, rapid sand filtration, preoxidation ($KMnO_4$), pH adjustment with $Ca(OH)_2$, and disinfection with chloramines
[3] Madrid	Santillana	4 m^3/s	Preoxidation-prechlorination (Cl_2 and Cl_2O), coagulation with PAC, flocculation, rapid sand filtration, preoxidation (O_3 or $KMnO_4$), pH adjustment with $Ca(OH)_2$, and disinfection with chloramines
[3] Madrid	El Bodonal	4 m^3/s	Preoxidation-prechlorination (HClO), coagulation with aluminium salts, flocculation, rapid sand filtration, preoxidation ($KMnO_4$), pH adjustment with $Ca(OH)_2$, and disinfection chloramines
[3] Madrid	Majadahonda	3.8 m^3/s	Preoxidation-prechlorination (NaClO and Cl_2O), coagulation with aluminium salts, flocculation, rapid sand filtration, preoxidation (O_3 and $KMnO_4$), GAC filtration, acidification and $Ca(OH)_2$ for pH adjustment, and disinfection with chloramines
[4] Barcelona	Sant Joan Despí y de Abrera	6.3 m^3/s	Preoxidation with Cl_2O, flocculation, sand filtration, filtration with activated carbon and chlorination disinfection, ultrafiltration (0.02 μm), ultraviolet disinfection and reverse osmosis/remineralization and chlorination
[4] Barcelona	Ter-Cardedeu	8 m^3/s	Coagulation, flocculation, filtration with activated carbon and chlorination disinfection
[5] San Cristobal de la Laguna	Montaña del Aire	0.10 m^3/s	Preoxidation (NaClO and Cl_2), flocculation-decantation, horizontal radial, or rectangular flux roughing filters, and chlorination
[5] San Cristobal de la Laguna	Los Baldíos	0.05 m^3/s	Preoxidation (NaClO and Cl_2), flocculation-decantation, horizontal radial, or rectangular flux roughing filters, and chlorination
[6] Las Palmas de Gran Canaria	EMALSA Las Palmas de Gran Canaria - Red Los Frailes	-	Disinfection, filtrating bed, membrane filtration (reverse osmosis), pH adjustment, final disinfection.

[6] Las Palmas de Gran Canaria	EMALSA Las Palmas de Gran Canaria - Red Las Brujas	-	Disinfection, filtrating bed, membrane filtration (reverse osmosis), pH adjustment, final disinfection.
[7] Cartagena	La Pedrera, Jacarilla, Alicante	4.1 m^3/s	Coagulation with aluminium sulfate and flocculation with ammonium derivatives. Sedimentation by Superpulsator®. Sand and activated carbon filtration. Prechlorination-disinfection with chlorine and chloramines
[8] Murcia	Contraparada	0.56 m^3/s	Preoxidation (Cl_2, Cl_2O and O_3), coagulation-flocculation, GAC filtration, post-ozonation, and disinfection
[8] Murcia	Torrealta	5.3 m^3/s	Preoxidation (Cl_2), coagulation-flocculation with aluminium sulphate, GAC and sand filtration, and disinfection

Table S2. Polymers and densities.

Polymer	**Density (g/cm^3)**
Polyethylene	0.95
Polypropylene	0.91
Polystyrene	1.04
Polyamide	1.07
Polyvinylchloride	1.38
Polyester	1.39
Acrylates	1.18
Polyurethane	1.26
Polychloroprene	1.23
Polylactic acid	1.26
Polytetrafluorethylene	2.20

Table S3. Particles found in procedural controls.

Location	Typology	micro-FTIR	Action taken in affected samples
[1]	Transparent fibre	Cellulose	Transparent cellulose was not considered artificial contaminant
[2]	Transparent fibre	Cellulose	Transparent cellulose was not considered artificial contaminant
	Black fibre	Not identified	This typology and colour do not match with any of the particles found in the affected sample
[3]	White fibre	Rayon	This typology and colour do not match with any of the particles found in the affected sample
	White fragment	Cellulose	White cellulose was not considered artificial contaminant
	Transparent fibre	Rayon	Transparent regenerated cellulose removed
[4]	White fibre	Wool	Natural material
[5]	Transparent fibre	Cellulose	Transparent cellulose was not considered artificial contaminant
[6]	Red fibre	Polyester	This typology and colour do not match with any of the particles found in the affected sample
	Blue fibre	Cellulose	Blue cellulose removed
	Transparent fibre	Rayon	Transparent regenerated cellulose removed
	Transparent fibre	Cellulose	Transparent cellulose was not considered artificial contaminant
[7]	Yellow fibre	Cellulose	This typology and colour do not match with any of the particles found in the affected sample
	White fragment	Not identified	-
	White fragment	Not identified	-
	White fibre	Cellulose	White cellulose was not considered artificial contaminant
	White fragment	Not identified	-
	Transparent fibre	Cellulose	Transparent cellulose was not considered artificial contaminant
[8]	Transparent fibre	Cellulose	Transparent cellulose was not considered artificial contaminant
Lab. control	Black fibre	Rayon	Black regenerated cellulose removed
Lab. control	Transparent fragment	Glass	-

Figure S1. Setup used for sampling.

Materials and methods. Particle size distributions.

As indicated in the body of the article, the abundance of plastic particles in environmental samples has been shown to follow a power law with size (Cozar et al., 2017; Kooi and Koelmans, 2019) because the fragmentation of a given plastic originates a high number of smaller particles. The relationship can be expressed by a probability density function denoted as *p(x)*:

$$p(x) = p(x \le X \le x + dx) \propto x^{-\alpha} \quad [1]$$

where X is the observed value and α the scaling parameter. The density function can be normalized to ensure that the probability of finding a fragment of any size is the unity. The reference size for it is usually the lower limit, x_{min}, to which the power law applies (if the power law is not followed below a certain size):

$$p(x) = \frac{\alpha - 1}{x_{\min}} \left(\frac{x}{x_{\min}} \right)^{-\alpha} \quad [2]$$

Then, provided $\alpha > 1$, the cumulative frequency distribution function (CFD), *P(x)*, can be easily derived:

$$P(x) = P(X \ge x) = \left(\frac{x}{x_{\min}} \right)^{-\alpha+1} \quad [3]$$

The scaling parameter has been interpreted as the dimension of a fractal fragmentation process that creates a given distribution and, when followed, the evidence of a scale invariant fragmentation mechanism. The scaling parameter also depends on the fragility (the probability of fragmentation) of the material (Turcotte, 1986). Estimating power-law distributions from experimental data is not trivial. Maximum likelihood estimation (MLE) is the method of choice to avoid large errors in the fitting of experimental data (Clauset et al. 2009). The method maximizes the likelihood of having observed a set of data x_1, x_2, ..., x_n under a certain statistical model (like the power law):

$$p(x_1, x_2, \cdots, x_n) = \prod \frac{\alpha - 1}{x_{\min}} \left(\frac{x}{x_{\min}} \right)^{-\alpha} \quad [4]$$

Taking logarithms and solving for the maximum likelihood, the estimator for the power law exponent can be easily derived:

$$\hat{\alpha} = \frac{n}{\sum \ln\left(\frac{x}{x_{\min}}\right)} + 1 \quad [5]$$

The uncertainty in parameter estimation can be obtained using a bootstrapping procedure that consists of generating multiple data sets from which the parameters $\hat{\alpha}$ and, if necessary, $\hat{x}_{min}$, are re-inferred. Details can be found elsewhere (Gillespie, 2015). The density function, *p(x)*, can be easily converted into a size distribution function, *n(x)*, as follows:

$$n(x) = N\ p(x) \quad [6]$$

Where *N* is total number (or number concentration) of particles and *n(x)* the number of particles with sizes between *x* and *x* + *dx*. Accordingly, the number and mass of particles between two sizes, x_1, and x_2 can be obtained as follows assuming spherical particles and an averaged particle density:

$$N_{x_1-x_2} = \int_{x_1}^{x_2} n(x)\,dx = N \int_{x_1}^{x_2} p(x)\,dx \quad [7]$$

$$M_{x_1-x_2} = \int_{x_1}^{x_2} \frac{\pi}{6} \rho\, x^3\, n(x)\,dx = \frac{\pi}{6} \rho\, N \int_{x_1}^{x_2} x^3\, p(x)\,dx \quad [8]$$

Integrating Eq. 8 combined with Eq. 2, the mass of particles between two sets of boundaries, (x_1, x_2) and (x_1', x_2') can be related by the following expression:

$$M_{x_1-x_2} = M_{x_1'-x_2'} \frac{x_2^{4-\alpha} - x_1^{4-\alpha}}{(x_2')^{4-\alpha} - (x_1')^{4-\alpha}} \quad [9]$$

Clauset A, Rohilla-Shalizi C, Newman MEJ. Power-Law distributions in empirical data. SIAM Review 2009; 51: 661-703.

Cózar A, Echevarría F, González-Gordillo JI, Irigoien X, Úbeda B, Hernández-León S, Palma ÁT, Navarro S, García-de-Lomas J, Ruiz A, Fernández-de-Puelles ML, Duarte CM. Plastic debris in the open ocean. 2014; 111: 10239-10244.

Gillespie CS. Fitting heavy tailed distributions: The poweRlaw package. Journal of Statistical Software 2015; 64: 1 - 16.

Kooi M, Koelmans AA. Simplifying microplastic via continuous probability distributions for size, shape, and density. Environmental Science & Technology Letters 2019; 6: 551-557.

Turcotte DL. Fractals and fragmentation. 1986; 91: 1921-1926.

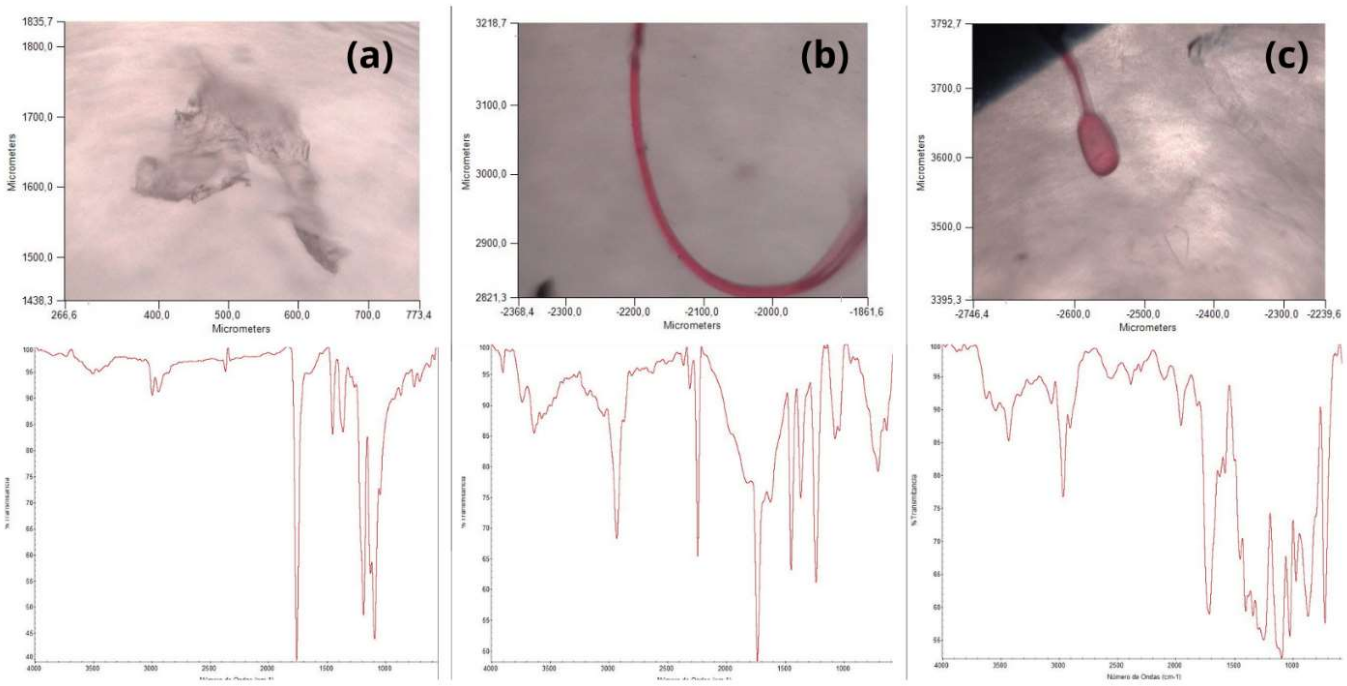

Figure S2. Images and micro-FTIR spectra of (a) PES fragment, (b) ACR fibre and (c) PLA fragment (PES: polyester; ACR: acrylic polymer; PLA: polylactic acid).

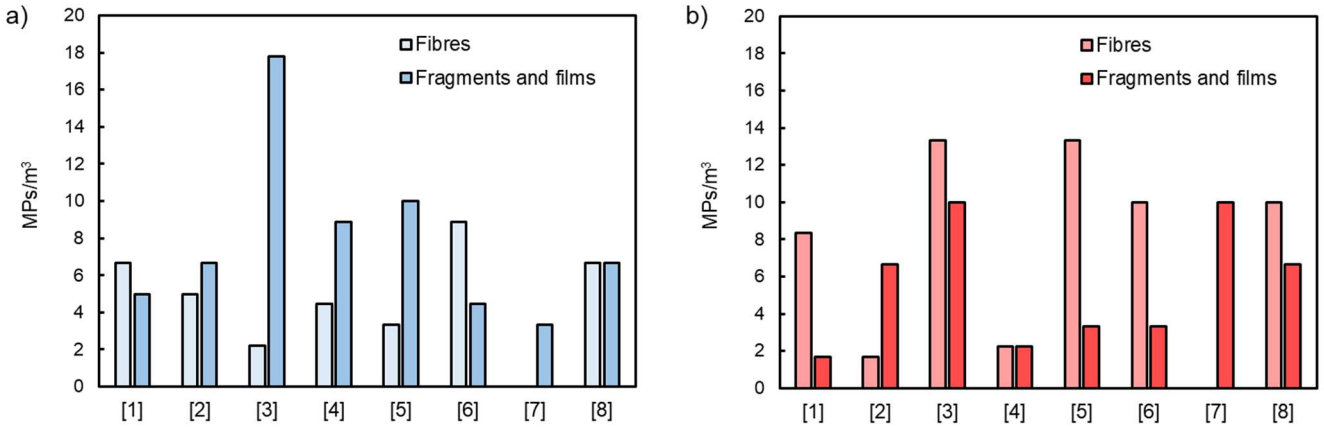

Figure S3. Number concentration of Microplastics (MPs). Fibres and fragments & films from the samples taken in May (a) and July (b).